

## Conductance and Permeation of Monovalent Cations through Depletion-Activated $\text{Ca}^{2+}$ Channels ( $I_{\text{CRAC}}$ ) in Jurkat T Cells

Albrecht Lepple-Wienhues and Michael D. Cahalan

Department of Physiology and Biophysics, University of California at Irvine, California 92717 USA

**ABSTRACT** We studied monovalent permeability of  $\text{Ca}^{2+}$  release-activated  $\text{Ca}^{2+}$  channels ( $I_{\text{CRAC}}$ ) in Jurkat T lymphocytes following depletion of calcium stores. When external free  $\text{Ca}^{2+}$  ( $[\text{Ca}^{2+}]_o$ ) was reduced to micromolar levels in the absence of  $\text{Mg}^{2+}$ , the inward current transiently decreased and then increased approximately sixfold, accompanied by visibly enhanced current noise. The monovalent currents showed a characteristically slow deactivation ( $\tau = 3.8$  and  $21.6$  s). The extent of  $\text{Na}^+$  current deactivation correlated with the instantaneous  $\text{Ca}^{2+}$  current upon readdition of  $[\text{Ca}^{2+}]_o$ . No conductance increase was seen when  $[\text{Ca}^{2+}]_o$  was reduced before activation of  $I_{\text{CRAC}}$ . With  $\text{Na}^+$  outside and  $\text{Cs}^+$  inside, the current rectified inwardly without apparent reversal below  $40$  mV. The sequence of conductance determined from the inward current at  $-80$  mV was  $\text{Na}^+ > \text{Li}^+ = \text{K}^+ > \text{Rb}^+ \gg \text{Cs}^+$ . Unitary inward conductance of the  $\text{Na}^+$  current was  $2.6$  pS, estimated from the ratios  $\Delta\sigma^2/\Delta I_{\text{mean}}$  at different voltages. External  $\text{Ca}^{2+}$  blocked the  $\text{Na}^+$  current reversibly with an  $\text{IC}_{50}$  value of  $4 \mu\text{M}$ .  $\text{Na}^+$  currents were also blocked by  $3$  mM  $\text{Mg}^{2+}$  or  $10 \mu\text{M}$   $\text{La}^{3+}$ . We conclude that  $I_{\text{CRAC}}$  channels become permeable to monovalent cations at low levels of external divalent ions. In contrast to voltage-activated  $\text{Ca}^{2+}$  channels, the monovalent conductance is highly selective for  $\text{Na}^+$  over  $\text{Cs}^+$ .  $\text{Na}^+$  currents through  $I_{\text{CRAC}}$  channels provide a means to study channel characteristics in an amplified current model.

### INTRODUCTION

A highly selective  $\text{Ca}^{2+}$  current in lymphoid and mast cells has been characterized and named  $I_{\text{CRAC}}$  to signify its activation by calcium release from intracellular stores (Lewis and Cahalan, 1989; Hoth and Penner, 1992; Zweifach and Lewis, 1993). Similar currents have also been described in a wide variety of nonexcitable cells, including rat basophilic leukemia (RBL) cells, macrophages, fibroblasts, thyrocytes, hepatocytes, a colonic epithelial cell line, *Xenopus* oocytes (for reviews see Fasolato et al., 1994; Lewis and Cahalan, 1995), and melanoma cell lines (Lepple-Wienhues and Cahalan, 1995). Different depletion-activated currents have been reported in vascular endothelium and epidermal cancer cells (Vaca and Kunze, 1994; Lückhoff and Clapham, 1994). They resemble the insect trp gene product in their poor selectivity for divalent over monovalent cations and single channel conductances in the  $10$  pS range.  $I_{\text{CRAC}}$  channels may represent a family of related  $\text{Ca}^{2+}$  entry channels that are involved in calcium homeostasis and signaling in diverse cell types. In T cells,  $I_{\text{CRAC}}$  provides the major  $\text{Ca}^{2+}$  influx pathway controlling basic cellular functions such as interleukin-2 gene expression, secretion, and cell proliferation (Zweifach and Lewis, 1993; Negulescu et al., 1994).  $I_{\text{CRAC}}$  currents are not voltage-operated, but open following depletion of intracellular  $\text{Ca}^{2+}$  stores.  $I_{\text{CRAC}}$  can be distinguished from other store-operated currents by its

high selectivity for  $\text{Ca}^{2+}$  and a unitary conductance well below  $1$  pS. In the absence of extracellular  $\text{Ca}^{2+}$  monovalent currents have been observed (Hoth and Penner, 1993; McDonald et al., 1993; Premack et al., 1994). Organic blockers of voltage-operated  $\text{Ca}^{2+}$  channels do not inhibit  $I_{\text{CRAC}}$  (Premack et al., 1994). Albeit nonspecific, the trivalent metals  $\text{La}^{3+}$  and  $\text{Gd}^{3+}$  are the most potent inhibitors (Hoth and Penner, 1993; Ross and Cahalan, 1995). Anomalous mole-fraction behavior for  $\text{Ba}^{2+}$  and  $\text{Ca}^{2+}$  has been described (Hoth, 1995). The mechanisms linking store-depletion and membrane current are still unknown. Involvement of small G proteins, a soluble messenger, and vesicular fusion have been suggested as activation pathways (Fasolato et al., 1993; Parekh et al., 1993; Randriamampita and Tsien, 1993; Somasundaram et al., 1995). Inactivation of the current has been shown to depend on intracellular  $\text{Ca}^{2+}$ , the type of chelator used in the pipette, and protein kinases (Hoth and Penner, 1993; Zweifach and Lewis, 1995a; Zweifach and Lewis, 1995b; Parekh and Penner, 1995). Noise analysis of  $\text{Ca}^{2+}$  currents has provided evidence for discretely gating channels in T cells with an estimated conductance of  $24$  fS in high external  $\text{Ca}^{2+}$ . This unitary conductance does not allow examination of single channel currents using available techniques. A conductance of  $24$  fs is extremely small for an ion channel, giving an estimate of  $>10,000$  channels per cell (Zweifach and Lewis, 1993).

In the present study we examined the permeation properties of  $I_{\text{CRAC}}$  channels for monovalent cations and the divalent block of monovalent currents. Macroscopic channel noise with  $\text{Na}^+$  as the charge carrier was analyzed to gain further insight into channel properties. A preliminary report has appeared (Lepple-Wienhues and Cahalan, 1996).

Received for publication 8 March 1996 and in final form 1 May 1996.

Address reprint requests to Dr. Michael D. Cahalan, Department of Physiology and Biophysics, University of California at Irvine, Irvine, CA 92717, Tel.: 714-824-7260; Fax: 714-824-8540; E-mail: mcahalan@uci.edu.

© 1996 by the Biophysical Society

0006-3495/96/08/787/08 \$2.00

## MATERIALS AND METHODS

### Cell culture

The human leukemia T-cell line Jurkat E6-1 was obtained from the American Type Culture Collection (Rockville, MD) and maintained in RPMI 1640/10% fetal calf serum media. The cells were passed twice weekly and kept at a low density ( $< 10^5$ /ml). For patch clamp experiments cells were allowed to settle on poly-D-lysine-coated coverslips.

### Solutions

Intracellular solutions contained (mM): 128 Cs aspartate, 10 Cs-*N*-[2-hydroxyethyl]piperazine-*N'*-[2-ethanesulfonic acid (HEPES, pH 7.2), and either 12 1,2-bis(2-aminophenoxy)ethane-*N,N,N',N'*-tetraacetic acid (BAPTA), 0.9 CaCl<sub>2</sub>, 3.16 MgCl<sub>2</sub> or 12 ethyleneglycol-bis( $\beta$ -Aminoethylether)*N,N,N',N'*-tetraacetic acid (EGTA), 0.7 CaCl<sub>2</sub>, 3.0 MgCl<sub>2</sub>. Free [Ca<sup>2+</sup>]<sub>i</sub> was 10 nM as measured using fura-2 ratios. 10  $\mu$ M inositol 1,4,5-trisphosphate (IP<sub>3</sub>) was added when indicated. The composition of external solutions is summarized in Table 1. External solutions used for permeability studies were prepared by titrating methanesulfonic acid using the hydroxide of the respective cation. EGTA stock solutions saturated with Ca<sup>2+</sup> and Mg<sup>2+</sup> were prepared using a pH-metric method (Neher, 1988). Free [Ca<sup>2+</sup>]<sub>o</sub> and [Mg<sup>2+</sup>]<sub>o</sub> levels were calculated using "Chelator" software (Theo J.M. Schoenmakers, University of Nijmegen, The Netherlands). NaOH and KOH were purchased from Fischer Scientific (Fair Lawn, NJ); LiOH and RbOH from Johnson Matthey Electronics (Ward Hill, MA); CsOH from Fluka Chemie (Buchs, Switzerland); charybdotoxin from Peptide Institute (Osaka, Japan); and HEPES from Calbiochem (La Jolla, CA). All other chemicals were purchased from Sigma (St. Louis, MO).

### Patch clamp recording

Whole-cell currents were recorded using an EPC-9 patch clamp amplifier (HEKA, Lambrecht, Germany). Patch pipettes were pulled from soft glass capillaries (Accu-fill 90 Micropets, Becton, Dickinson and Co., Parsippany, NJ), sylgard coated (Dow Corning Corp., Midland, MI), and fire-polished to 2-4 M $\Omega$  resistance in Ringer. Amplifier control and data

recording were performed using a Macintosh Quadra 700 microcomputer (Apple Computer, Cupertino, CA). Data were sampled at 5-10 kHz and digitally filtered at 0.5 kHz for analysis and display. Fast and slow capacitive transients were canceled using the compensation circuitry of the EPC-9. Series resistance (5-10 M $\Omega$ ) was not compensated. Voltage was corrected for liquid junction potentials. Fast solution exchange was achieved using a mobile linear array of wide-tipped puffer pipettes. The solution exchange time estimated from the block of Na<sup>+</sup> current by Ca<sup>2+</sup> and the removal of block when Ca<sup>2+</sup> was washed out was  $< 150$  ms. The reference electrode was connected using a Ringer agar bridge. All experiments were performed at room temperature (22-25°C). For noise analysis, data were sampled at 5 kHz and digitally low-pass-filtered at 1 kHz. To eliminate low frequency components ( $< 10$  Hz) from power spectra, a third-order polynomial fit was performed on continuous traces and subtracted. To obtain current variance, 500-ms intervals of traces were digitally low-pass-filtered at 700 Hz. During this sampling interval, the mean current changed by  $< 10\%$ . Analysis was performed using the programs Pulse (HEKA, Lambrecht, Germany) and Igor Pro (Wavemetrics, Lake Oswego, Oregon).

## RESULTS

### The depletion-activated channel is permeable to Na<sup>+</sup> when external divalent cations are removed

Following activation of I<sub>CRAC</sub> by depletion of intracellular Ca<sup>2+</sup> stores, withdrawal of external divalent ions revealed a monovalent conductance much larger than that carried by Ca<sup>2+</sup> ions. This conductance was observed only when the concentration of external divalent cations was reduced to micromolar levels or lower. Fig. 1 shows a typical experiment. Intracellular Ca<sup>2+</sup> stores were depleted using 10  $\mu$ M IP<sub>3</sub> and 12 mM BAPTA in the pipette. [Ca<sup>2+</sup>]<sub>o</sub> was varied as indicated, and Na<sup>+</sup> was the only monovalent cation present in the low [Ca<sup>2+</sup>]<sub>o</sub> solution, which contained no Mg<sup>2+</sup>. I<sub>CRAC</sub> developed within 20 s of break-in as IP<sub>3</sub> reduced the Ca<sup>2+</sup> content of the stores. When [Ca<sup>2+</sup>]<sub>o</sub> was

TABLE 1 External solutions

Solution	[Na <sup>+</sup> ]	[K <sup>+</sup> ]	[X <sup>+</sup> ]	[Ca <sup>2+</sup> ] (total)	pCa (free)	[Mg <sup>2+</sup> ] (total/free)	[Cl <sup>-</sup> ]	[CH <sub>3</sub> SO <sub>3</sub> <sup>-</sup> ]	[Chelator]
1	120	5	—	20	1.7	—/—	165	—	—
2	160	5	—	2	2.7	—/—	169	—	—
3	160	5	—	0.1	4	—/—	165	—	—
4	160	5	—	1.8	5	—/—	165	—	2 HEDTA
5	160	5	—	1.8	6	—/—	165	—	2 EGTA
6	160	5	—	0.88	7	—/—	165	—	2 EGTA
7	160	5	—	0.15	8	—/—	165	—	2 EGTA
8	160	5	—	1.2	5	3.7/3	165	—	2 HEDTA
9	160	5	—	0.25	6	4.4/3	165	—	2 HEDTA
10	—	—	120 NMG <sup>+</sup>	20	1.7	—/—	2	158	—
11	120	—	—	20	1.7	—/—	2	158	—
12	160	—	—	1.8	6	—/—	2	158	2 EGTA
13	—	—	160 Rb <sup>+</sup>	1.8	6	—/—	2	158	2 EGTA
14	—	—	160 Cs <sup>+</sup>	1.8	6	—/—	2	158	2 EGTA
15	—	—	160 K <sup>+</sup>	1.8	6	—/—	2	158	2 EGTA
16	—	—	160 Li <sup>+</sup>	1.8	6	—/—	2	158	2 EGTA
17	—	—	160 NMG <sup>+</sup>	1.8	6	—/—	2	158	2 EGTA
18	—	—	160 NMG <sup>+</sup>	—	~5	—/—	2	158	—

Concentrations in mM. All solutions contained 10 mM HEPES and 5 mM glucose, and were titrated to pH 7.4 (CH<sub>3</sub>SO<sub>3</sub><sup>-</sup> = methanesulphonate, NMG<sup>+</sup> = N-methyl-D-glucamine, HEDTA = N-hydroxyethyl-ethylenediamine-triacetic acid). 0.1  $\mu$ M charybdotoxin was present in K<sup>+</sup>- and Rb<sup>+</sup>-containing solutions to block current through K<sup>+</sup> channels.

reduced to 1 and 10  $\mu\text{M}$ , a larger inward  $\text{Na}^+$  current was revealed that inactivated. In five similar experiments, the ratio of  $\text{Na}^+$  to  $\text{Ca}^{2+}$  current averaged  $6.4 \pm 1.3$  ( $\text{pCa} = 6$  vs.  $\text{pCa} = 1.7$ ), with a maximal  $\text{Na}^+$  conductance of  $448 \pm 67$  pS ( $n = 5$ ). Readdition of 20 mM  $[\text{Ca}^{2+}]_o$  enabled the smaller  $\text{Ca}^{2+}$  current to redevelop. The I-V relations of both  $\text{Na}^+$  and  $\text{Ca}^{2+}$  currents were strongly inward rectifying (Fig. 1 B) and no measurable outward current developed during inactivation. These results suggest that  $I_{CRAC}$  channels become permeable to  $\text{Na}^+$  when  $\text{Ca}^{2+}$  is reduced to the micromolar range, a property shared with voltage-gated  $\text{Ca}^{2+}$  channels (Hess and Tsien, 1984; Almers et al., 1984).

### Inactivation of $\text{Na}^+$ currents correlates with subsequent reactivation of $\text{Ca}^{2+}$ currents

When  $\text{IP}_3$  was omitted from the pipette solution, passive store depletion was slow allowing several solution changes before induction of the current. As shown in Fig. 2A,  $\text{Na}^+$  current could not be evoked when  $[\text{Ca}^{2+}]_o$  was removed before activation of the  $\text{Ca}^{2+}$  current.  $\text{Ca}^{2+}$  and  $\text{Na}^+$  currents were induced in parallel by slow passive store depletion with a strong correlation between the magnitudes of  $\text{Ca}^{2+}$  currents and peak  $\text{Na}^+$  currents (Fig. 2A, inset).

$\text{Na}^+$  currents activated by stores depletion showed a characteristically slow inactivation (Figs. 1 A and 2 A, see also Hoth and Penner, 1993), resembling the kinetics of slow  $\text{Ca}^{2+}$  dependent activation of depletion-activated  $\text{Ca}^{2+}$  currents (Zweifach and Lewis, 1996). Slow inactivation of  $\text{Na}^+$  currents in the virtual absence of  $\text{Ca}^{2+}$  may therefore represent a reversal of the slow activation of  $\text{Ca}^{2+}$  currents, which is known to depend on the extracellular  $\text{Ca}^{2+}$  concentration. To test this hypothesis, we varied the duration of  $[\text{Ca}^{2+}]_o$  reduction, allowing for different degrees of  $\text{Na}^+$  current inactivation. When external  $\text{Ca}^{2+}$  was raised before the  $\text{Na}^+$  currents were completely inactivated, the subsequent instantaneous  $\text{Ca}^{2+}$  current (upon readmission of  $\text{Ca}^{2+}$ ) was larger. When  $\text{Na}^+$  currents in low  $[\text{Ca}^{2+}]_o$  inactivated completely, the instantaneous  $\text{Ca}^{2+}$  current was reduced. Fig. 2 B shows a clear correlation between the instantaneous  $\text{Ca}^{2+}$  current and the extent of  $\text{Na}^+$  current inactivation. Both the inactivation of  $\text{Na}^+$  currents and the subsequent activation of  $\text{Ca}^{2+}$  currents could be well fitted using double exponentials. These parallels in the development and inactivation of  $\text{Na}^+$  and  $\text{Ca}^{2+}$  current provide strong evidence that both currents are carried through  $I_{CRAC}$  channels.

$\text{Ca}^{2+}$  currents through  $I_{CRAC}$  channels undergo rapid inactivation within several tens of ms, probably because of binding of  $\text{Ca}^{2+}$  to sites close to the inner channel mouth (Zweifach and Lewis, 1995a). This inactivation depends on the type of the intracellular chelator and is also seen in RBL cells (Hoth and Penner, 1993). As shown in Fig. 2 C, the  $\text{Na}^+$  current does not undergo rapid inactivation as seen with the  $\text{Ca}^{2+}$  current, providing further evidence that this rapid inactivation depends on  $\text{Ca}^{2+}$  entry.

### Monovalent selectivity sequence

Current-voltage relationships illustrated in Fig. 3 provide further evidence for  $\text{Na}^+$  as the charge carrier with micromolar concentration of external divalent cations. The positive reversal potential indicates a poor permeability to  $\text{Cs}^+$  (Figs. 1 B and 3 A). In most cells when external  $\text{Na}^+$  was replaced by  $\text{Cs}^+$ , the conductances for  $\text{NMG}^+$  and  $\text{Cs}^+$  were indistinguishably low within the studied voltage range. However, some cells displayed an additional nonspecific cation conductance with similar permeability for  $\text{Cs}^+$  and  $\text{Na}^+$ . This "leak" conductance showed linear I-V relations and lacked the characteristically slow inactivation. Neglecting cells with a large leak component, we alternated  $[\text{Ca}^{2+}]_o$  between 20 mM and 1  $\mu\text{M}$  to determine the inactivating component of monovalent whole cell currents. Fig. 3 B shows membrane currents in solutions containing  $\text{Na}^+$ ,  $\text{Li}^+$ ,  $\text{K}^+$ , and  $\text{NMG}^+$  as the only cations at 1  $\mu\text{M}$   $[\text{Ca}^{2+}]_o$ . Evidently, the channels are highly selective for  $\text{Na}^+$  over  $\text{Cs}^+$  even in the virtual absence of divalent cations. The sequence of conductance estimated from inward current

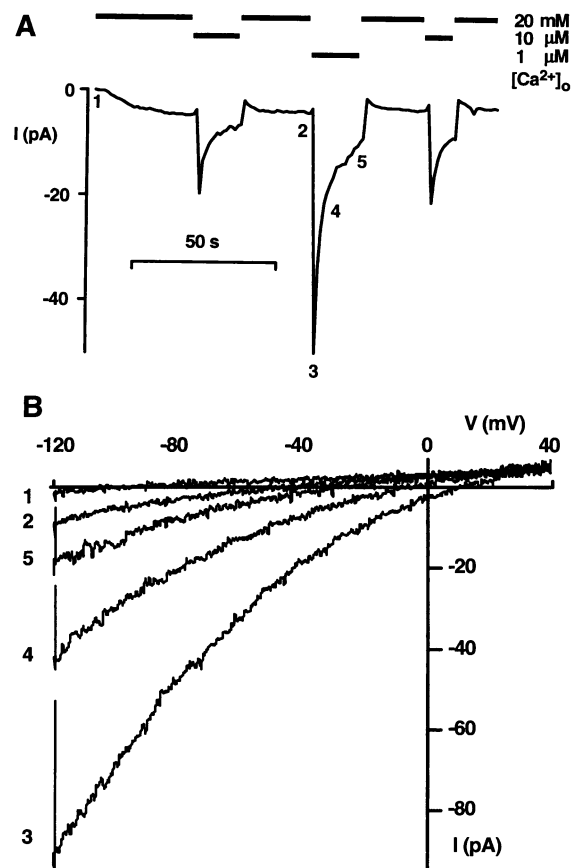
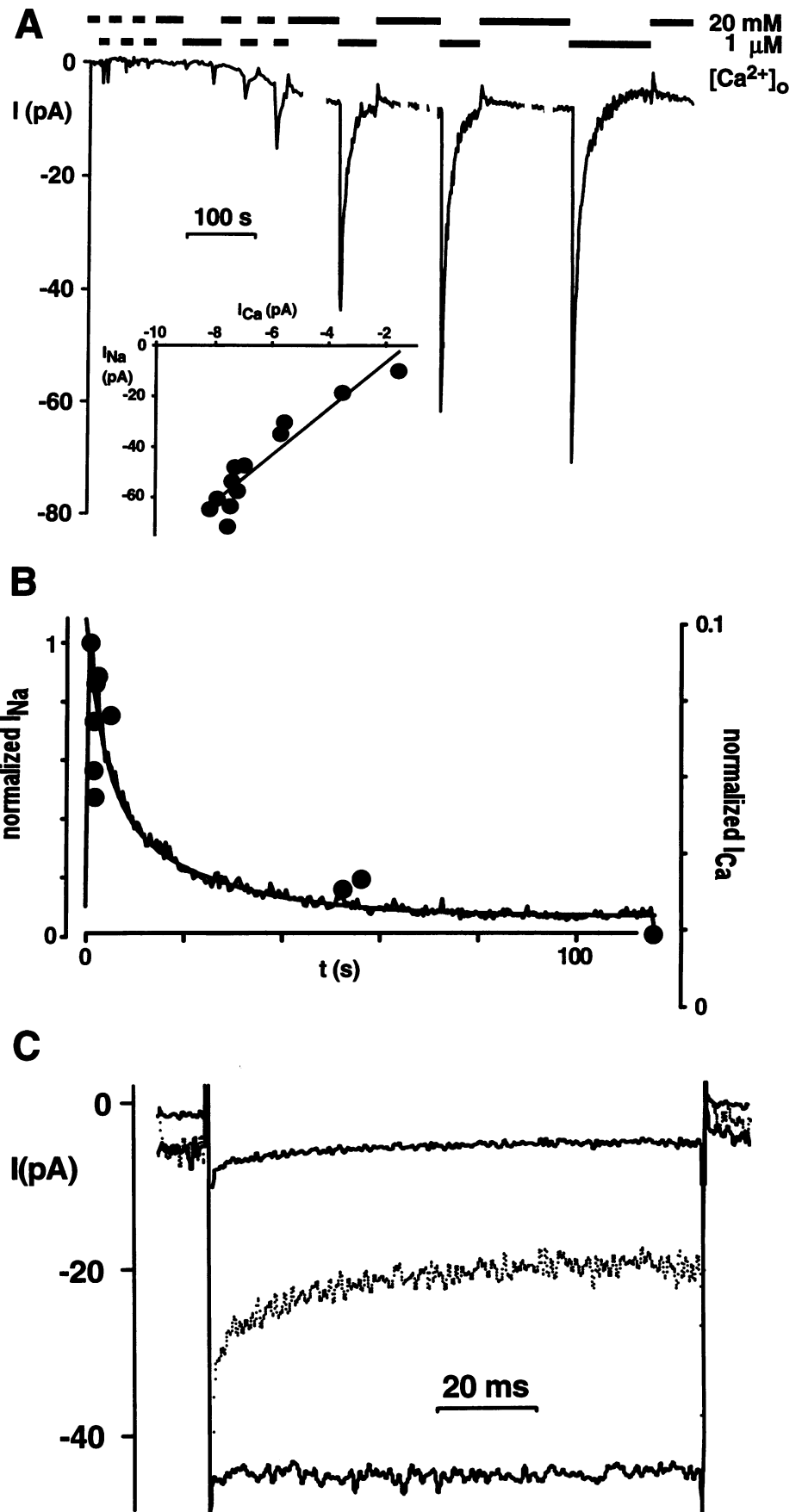


FIGURE 1 Inward current induced by  $\text{IP}_3$ -mediated store depletion at 1  $\mu\text{M}$ , 10  $\mu\text{M}$  and 20 mM  $[\text{Ca}^{2+}]_o$ . (A) Following activation of  $I_{CRAC}$  in 20 mM  $[\text{Ca}^{2+}]_o$ , a  $\text{Na}^+$  current is unmasked by lowering  $[\text{Ca}^{2+}]_o$  to 1 or 10  $\mu\text{M}$ . Inward currents at  $-80$  mV were obtained using 200-ms voltage ramps repeated at 1 s intervals (holding potential  $-20$  mV). (B) Ramp currents at the indicated times were filtered at 700 Hz and not leak subtracted. The pipette contained 12 mM BAPTA (Solutions 1, 4 and 5).

**FIGURE 2** Development and inactivation of  $\text{Na}^+$  and  $\text{Ca}^{2+}$  current through  $I_{\text{CRAC}}$  channels. (A) Parallel induction of  $\text{Na}^+$  and  $\text{Ca}^{2+}$  currents following slow passive store depletion (12 mM BAPTA, no  $\text{IP}_3$ ). (*inset*)  $\text{Ca}^{2+}$  current plateaus are plotted against subsequent peak  $\text{Na}^+$  currents, showing the simultaneous induction of both currents. Note the lack of  $\text{Na}^+$  current when  $[\text{Ca}^{2+}]_o$  is lowered before store depletion. Spontaneous small inward current spikes were seen in some cells (cf. Zweifach and Lewis, 1993). Short pulses of  $1 \mu\text{M}$   $[\text{Ca}^{2+}]_o$  could not be resolved at this time scale and were left out for clarity. Currents were obtained using pulses of 100 ms duration from  $-20$  to  $-100$  mV every 400 ms. Six pulses obtained immediately after disruption of the membrane were averaged and subtracted. (B) Inactivation of  $\text{Na}^+$  currents determines instantaneous  $\text{Ca}^{2+}$  currents. When  $[\text{Ca}^{2+}]_o$  was raised back to 20 mM following variable intervals of  $1 \mu\text{M}$   $[\text{Ca}^{2+}]_o$ , the subsequent instantaneous  $\text{Ca}^{2+}$  current ( $\bullet$ ) closely followed the extent of  $\text{Na}^+$  current inactivation. Approximately 20% of the instantaneous  $\text{Ca}^{2+}$  current remained following prolonged  $\text{Na}^+$  current inactivation. Current data were fitted using double exponential functions with time constants and amplitude coefficients (in parentheses) normalized to peak  $\text{Na}^+$  current:  $\tau = 3.8$  s (0.58) and 21.6 s (0.42) for the inactivation of the  $\text{Na}^+$  current and  $\tau = 1.2$  s (0.11) and 14.8 s (0.05) for the activation of the  $\text{Ca}^{2+}$  current (not shown).  $\text{Ca}^{2+}$  currents are shown at a magnified scale with an offset of 0.02. (C) Rapid inactivation is seen with  $\text{Ca}^{2+}$  (*upper trace*), but not  $\text{Na}^+$  (*lower trace*) as the charge carrier. 100-ms pulses from  $-20$  to  $-120$  mV were applied. Four subsequent pulses were averaged and leak-subtracted using pulses before activation of the current. The dashed trace shows the  $\text{Ca}^{2+}$  current magnified four times (solutions 10 and 12).



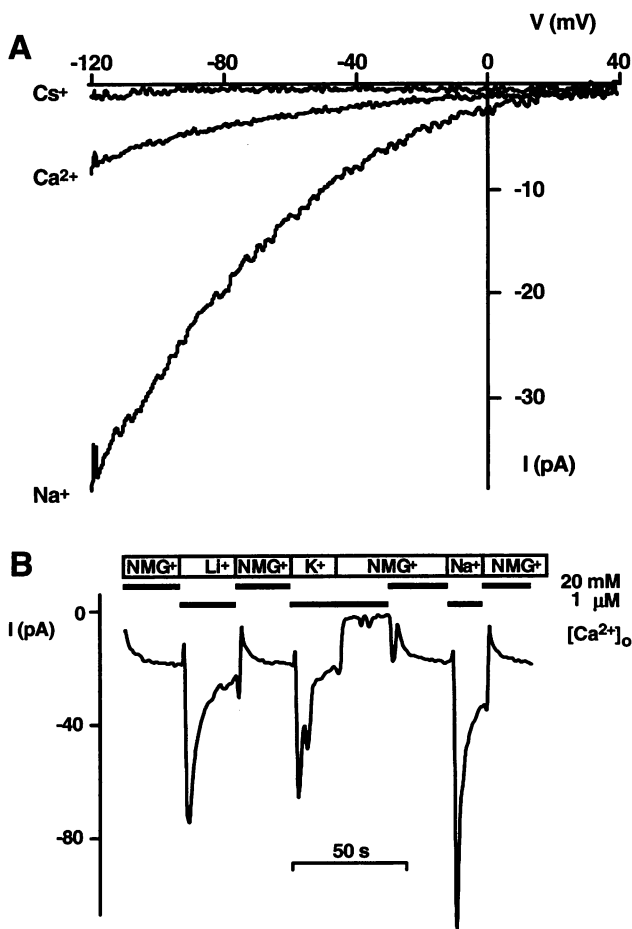


FIGURE 3 Monovalent current through  $I_{CRAC}$  channels. (A) Whole cell currents in response to voltage ramps ( $-120$  to  $40$  mV for a duration of  $200$  ms, holding potential  $-20$  mV). Currents in  $20$  mM  $Ca^{2+}$  (with  $120$  mM  $NMG^+$ ) and  $160$  mM  $Na^+$  ( $10^{-6}$  M  $Ca^{2+}$ ) outside were inwardly rectifying and did not reverse up to  $40$  mV.  $160$  mM  $Cs^+$  ( $10^{-6}$  M  $Ca^{2+}$ ) carried only a minuscule inward current. Leak current was determined with  $160$  mM  $NMG^+$  ( $10^{-6}$  M  $Ca^{2+}$ ) and subtracted (solutions 10, 12, and 17). (B) Conductance for  $Na^+$ ,  $Li^+$ ,  $K^+$ , and  $NMG^+$  seen as inward currents at  $-80$  mV. The slowly activating current with the  $NMG^+$  solution containing  $20$  mM  $Ca^{2+}$  was carried by  $Ca^{2+}$ . The short transient before activation of the  $Ca^{2+}$  current in  $NMG^+$  solution is an artifact. Ramps obtained before current activation were subtracted (solutions 10, 12, and 15–17).

magnitudes is:  $P_{Na} > P_{Li} = P_K > P_{Rb} \gg P_{Cs} \geq P_{NMG}$ . We were unable to determine reversal potentials due to 1) the small  $Cs^+$  currents, 2) inward rectification of the current, and 3) the tendency of seals to become leaky when the voltage was raised  $>40$  mV at micromolar calcium levels.

### Block of $Na^+$ current

$Na^+$  currents were blocked by extracellular  $Ca^{2+}$  in a dose-dependent manner. Fig. 4 A shows a typical experiment with transient  $Na^+$  currents at different  $[Ca^{2+}]_o$  levels. Similar experiments with  $[Ca^{2+}]_o$  varying from submicromolar to millimolar levels are summarized in Fig. 4 B. Inactivating  $Na^+$  currents become smaller at higher  $[Ca^{2+}]_o$  levels,

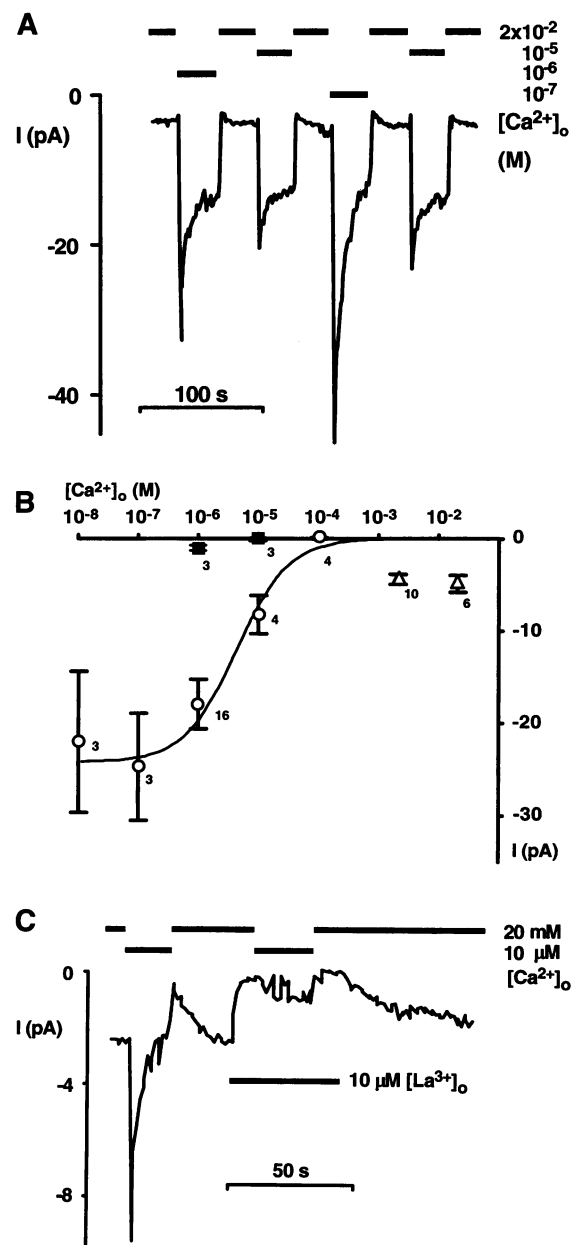


FIGURE 4 Block of  $Na$  current through  $I_{CRAC}$  channels by  $Ca^{2+}$  and  $La^{3+}$ . (A) Inactivating  $Na^+$  currents at different  $[Ca^{2+}]_o$  levels. Currents were activated using  $10 \mu M$   $IP_3$  in the pipette (Solutions 1 and 4–6, ramp currents at  $-80$  mV measured as in Fig. 1). (B) Inward current at  $-80$  mV as a function of  $[Ca^{2+}]_o$ . The inactivating component of the  $Na^+$  current (○) was obtained by subtracting the steady-state current from the peak current. The line represents a Michaelis-Menten fit assuming a Hill coefficient of 1.  $Mg^{2+}$  in the bath ( $3$  mM) blocked the current at  $[Ca^{2+}]_o \leq 10^{-5}$  M (■). Steady-state  $Ca^{2+}$  currents were plotted for comparison (Δ) (Solutions 1–9). (C)  $La^{3+}$  blocks  $Ca^{2+}$  currents and inactivating  $Na^+$  currents reversibly.  $Na^+$  is the main cation throughout the experiment. The low  $[Ca^{2+}]_o$  solution contains no chelators to avoid interactions with  $La^{3+}$  (ramp currents at  $-80$  mV, solutions 10 and 18).

following an apparent simple one to one stoichiometry with an  $IC_{50}$  of  $4 \mu M$  ( $pCa = 5.4$ , Hill coefficient of 1). At  $pCa = 4$  no measurable inactivating  $Na^+$  current could be observed. If  $[Ca^{2+}]_o$  was raised further, a slowly activating

$\text{Ca}^{2+}$  current was seen without slow inactivation (see above). The  $\text{Ca}^{2+}$  current was not altered by changing extracellular  $\text{Na}^+$  concentration (not shown, cf. Hoth and Penner, 1993).  $\text{Na}^+$  currents at  $\text{pCa} \geq 5$  were completely blocked by 1 mM extracellular  $\text{Mg}^{2+}$ . 10  $\mu\text{M}$   $\text{La}^{3+}$  blocked the  $\text{Ca}^{2+}$  current as well as the inactivating  $\text{Na}^+$  current reversibly (Fig. 4 C).  $\text{Na}^+$  currents were not altered when 1  $\mu\text{M}$  tetrodotoxin was added (not shown).

### Noise analysis of $\text{Na}^+$ currents

Fig. 5 A shows a continuous current recording from a cell voltage clamped at  $-60$  mV. When  $[\text{Ca}^{2+}]_o$  was rapidly reduced from 20 mM to 1  $\mu\text{M}$ , a transient decline of current was followed by the development of a large inward current. The increase of mean current was accompanied by fluctuations seen as macroscopic current noise (Fig. 5 B). We determined mean current and current variance at different holding voltages in a series of 500-ms intervals during the slow inactivation phase, as shown in Fig. 5 C. Assuming a low open probability, the single channel conductance of  $I_{\text{CRAC}}$  channels carrying  $\text{Na}^+$  current, as estimated from the slope in Fig. 5 C, is 2.6 pS. Power spectra were obtained from traces as shown in Fig. 5, A and B. Fig. 5 D shows the spectra of the  $\text{Na}^+$  current fitted by eye using a single Lorentzian

$$S(f) = S(0)/[1 + (f/f_c)^2]$$

where  $S(f)$  is the spectral current density at a given frequency  $f$  and  $f_c$  is the corner frequency. The corner frequency was  $f_c = 150$  Hz, and the total variance  $S(0) \times \pi \times f_c/2 = 21$   $\text{pA}^2$ .

### DISCUSSION

$I_{\text{CRAC}}$  channels are activated by depletion of intracellular  $\text{Ca}^{2+}$  stores and underlie the  $\text{Ca}^{2+}$  influx essential for sustained  $\text{Ca}^{2+}$  signaling, gene expression, and proliferation of T lymphocytes (Lewis and Cahalan, 1989; Zweifach and Lewis, 1993; Negulescu et al., 1994). In most cells, these

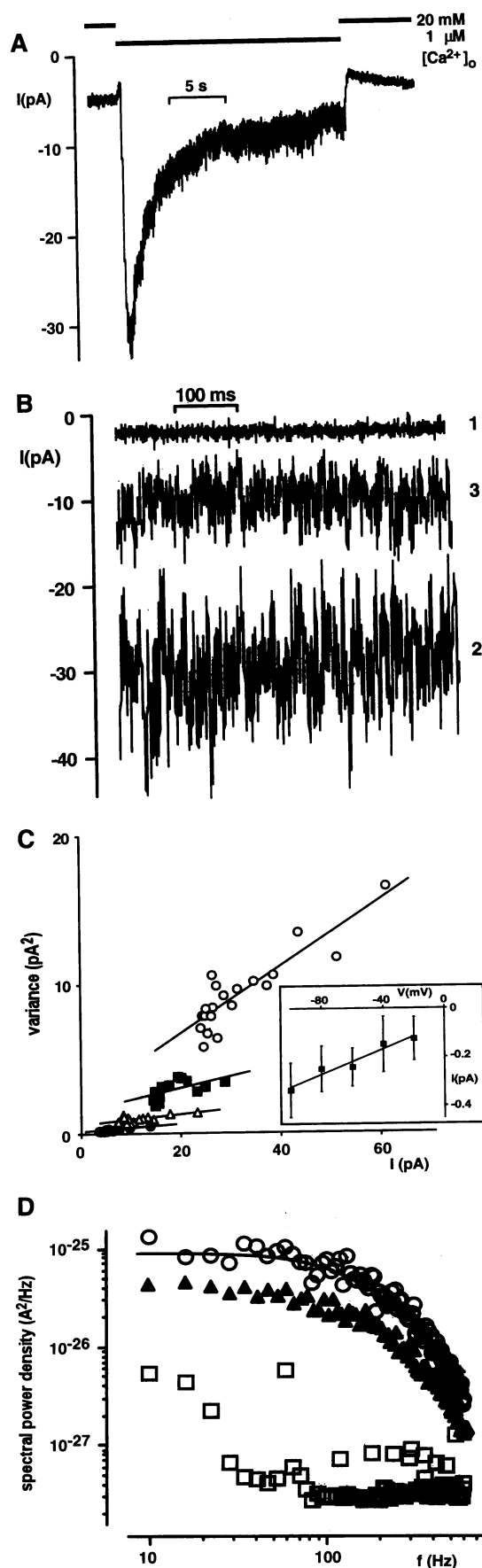


FIGURE 5 Noise analysis of  $\text{Na}^+$  current through  $I_{\text{CRAC}}$  channels. (A) Continuous recording of inward current at  $-60$  mV holding potential.  $[\text{Ca}^{2+}]_o$  is altered between 20 mM and 1  $\mu\text{M}$  as indicated (solutions 11 and 12). Note the slow activation/inactivation. (B) Current noise as seen during  $\text{Na}^+$  current inactivation. 1 kHz filtering. Traces 1–3 show  $\text{Ca}^{2+}$  current, peak  $\text{Na}^+$  current, and partially inactivated  $\text{Na}^+$  current before, 1 s and 22 s after removal of  $[\text{Ca}^{2+}]_o$ , at  $-80$  mV. (C) Variance versus mean current plotted at different holding potentials ( $\circ$   $-100$ ,  $\blacksquare$   $-80$ ,  $\blacktriangle$   $-60$ , and  $\bullet$   $-20$  mV, same cell as in A). Current traces were analyzed during inactivation of the  $\text{Na}^+$  current ( $\text{pCa} = 6$ ). The inset shows single-channel amplitudes estimated from slopes in the main panel ( $n = 4$  cells). (D) Power spectral analysis of  $\text{Na}^+$  currents. Power spectra were analyzed in a continuous current trace before ( $\circ$ ) and after inactivation of the  $\text{Na}^+$  current ( $\blacktriangle$ ) and with  $\text{Ca}^{2+}$  blocking the  $\text{Na}^+$  current ( $\square$ ). The fit is a single Lorentzian described in the text ( $f_c = 150$  Hz). Similar results were obtained in four cells.

channels mediate the immunoglobulin E response triggering secretion (Zhang and McCloskey, 1995).

Here we demonstrate that the  $I_{\text{CRAC}}$  channel, once activated, is permeable to  $\text{Na}^+$  upon removal of extracellular  $\text{Ca}^{2+}$ . Several lines of evidence argue for the observed  $\text{Na}^+$  current passing through the depletion-activated  $\text{Ca}^{2+}$  channel  $I_{\text{CRAC}}$ . 1)  $\text{Ca}^{2+}$  and  $\text{Na}^+$  currents are the only measurable currents in store-depleted Jurkat cells when using  $\text{Cs}^+$  as the main internal cation. T cells are electrically very tight, with only a limited number of ion channel types. The two prevailing  $\text{K}^+$  channels and the swelling activated chloride channel do not contribute current using the described patch clamp protocol. Involvement of voltage activated  $\text{Na}^+$  channels was ruled out using tetrodotoxin. 2)  $\text{Na}^+$  and  $\text{Ca}^{2+}$  currents developed in parallel when stores were depleted slowly (Fig. 2 A).  $\text{Na}^+$  currents as described here were never observed before store depletion took effect. 3) Slow inactivation of  $\text{Na}^+$  currents reduced the subsequent magnitude of  $\text{Ca}^{2+}$  currents (Fig. 2 B). When  $\text{Ca}^{2+}$  was raised after a short period of  $\text{Na}^+$  current, the instantaneous  $\text{Ca}^{2+}$  current was large. When, in contrast, the  $\text{Na}^+$  current was allowed to inactivate fully, the subsequent  $\text{Ca}^{2+}$  current reactivated slowly starting with only a small instantaneous current. These data suggest that slow  $\text{Ca}^{2+}$ -dependent activation of  $\text{Ca}^{2+}$  currents is reversed at low external  $\text{Ca}^{2+}$  concentrations, seen as slow inactivation of  $\text{Na}^+$  currents. 4) The trivalent rare earth  $\text{La}^{3+}$  is a potent blocker of both the  $\text{Ca}^{2+}$  and the  $\text{Na}^+$  current. We therefore postulate, that the  $\text{Na}^+$  current at low  $\text{Ca}^{2+}$  concentrations and the  $\text{Ca}^{2+}$  current in the presence of millimolar  $\text{Ca}^{2+}$  levels are conducted by the same channel.

The permeation of  $\text{Na}^+$  provides strong evidence that the depletion-activated current is mediated by an ion channel, in agreement with previous reports (Hoth and Penner, 1992; Zweifach and Lewis, 1993; Hoth and Penner, 1993). The unitary  $\text{Na}^+$  current estimated from variance and mean currents is rather large for an ion carrier, and both the macroscopically visible noise and the Lorentzian shape of the power spectrum are typical for a gated channel. A large shift in reversal potential was observed when extracellular  $\text{Ca}^{2+}$  was lowered using an intracellular potassium glutamate solution in mast cells (Hoth and Penner, 1993). This was probably due to an outward  $\text{K}^+$  current through  $I_{\text{CRAC}}$  channels. Using  $\text{Cs}^+$  as the main internal cation, no outward current developed and the reversal potential of  $\text{Na}^+$  currents remained positive during inactivation (Fig. 1 B). We find that the unitary conductance of  $I_{\text{CRAC}}$  channels with  $\text{Na}^+$  as the charge carrier is 2.6 pS when external  $\text{Ca}^{2+}$  is kept at 1  $\mu\text{M}$ . This value is  $\sim 100$  times the estimated single channel conductance for  $\text{Ca}^{2+}$  currents (Zweifach and Lewis, 1993), and therefore in a more common range for most ion channels. Whole cell  $\text{Na}^+$  currents, however, are only  $\sim 6$  times larger. The apparent discrepancy between increases in unitary and whole cell conductance could be explained by the observed  $\text{Ca}^{2+}$ -dependent activation of  $I_{\text{CRAC}}$  channels, assuming a current component that inactivates within the solution exchange time when reducing extracellular  $\text{Ca}^{2+}$ .

This would produce an underestimate of the initial  $\text{Na}^+$  current. However, even the faster component of the slow inactivation ( $\tau = 3.8$  s) would not account for a large error. A second possible explanation involves a likely change in channel kinetics induced by low  $[\text{Ca}^{2+}]_o$ . The open probability of the channels could be reduced under these conditions. In fact, spectral analysis reveals a faster channel gating. At 1  $\mu\text{M}$   $[\text{Ca}^{2+}]_o$ , the corner frequency of the  $\text{Na}^+$  current spectrum is three times greater than the corner frequency of  $\text{Ca}^{2+}$  currents (45 Hz, Zweifach and Lewis, 1993). The number of open single channels obtained from whole cell  $\text{Na}^+$  conductance and single channel conductance is 150–200 per cell. This number is roughly 50 times smaller than previous estimates from  $\text{Ca}^{2+}$  current measurements and may underestimate the total channel number due to a small open probability. On the other hand, analysis of the macroscopic  $\text{Na}^+$  current noise is probably more accurate than the analysis of extremely small  $\text{Ca}^{2+}$  current fluctuations.

Ion permeation of  $I_{\text{CRAC}}$  channels and voltage-gated  $\text{Ca}^{2+}$  channels share the property of monovalent permeation in low divalent concentration. However, there are some striking differences in ion selectivity properties, both for monovalents and divalents. Divalent ion selectivity of  $I_{\text{CRAC}}$  channels is unusual when compared with other  $\text{Ca}^{2+}$  channels. The conductance sequence has been described as  $\text{Ca}^{2+} > \text{Ba}^{2+} \approx \text{Sr}^{2+} \gg \text{Mn}^{2+}$  (Hoth and Penner, 1993). Newer findings have shown a higher  $\text{Ba}^{2+}$  permeability of  $I_{\text{CRAC}}$  channels in mast and RBL cells when compared with Jurkat cells, a strong voltage dependence of the  $I_{\text{Ba}}/I_{\text{Ca}}$  ratio and anomalous mole fraction behavior for  $\text{Ca}^{2+}/\text{Ba}^{2+}$  mixtures (Hoth, 1995). Our data suggest a high affinity site in the selectivity filter, which can be occupied by a single  $\text{Ca}^{2+}$  ion. This is in good agreement with findings in voltage-activated  $\text{Ca}^{2+}$  channels (Almers et al., 1984; Hess and Tsien, 1984), with the affinity for  $\text{Ca}^{2+}$  being slightly lower in  $I_{\text{CRAC}}$  channels (4 vs.  $\sim 1$   $\mu\text{M}$ ). Recently, a single high-affinity  $\text{Ca}^{2+}$  binding site in the outer pore of voltage-gated  $\text{Ca}^{2+}$  channels has been demonstrated using site-directed mutagenesis (Ellinor et al., 1995). However, the complex and multiple actions of  $\text{Ca}^{2+}$  on  $I_{\text{CRAC}}$  channels demand caution when interpreting the apparent stoichiometry. As in voltage-activated  $\text{Ca}^{2+}$  channels, the existence of anomalous mole fraction behavior and the increase of  $\text{Ca}^{2+}$  current over the range of 0.1 to 10 mM strongly suggest the existence of additional  $\text{Ca}^{2+}$  binding sites with lower affinity within the pore.  $\text{Mg}^{2+}$  blocks monovalent currents; this is also seen in voltage-gated  $\text{Ca}^{2+}$  channels (Almers et al., 1984; Fukushima and Hagiwara, 1985). However, we find an unusual monovalent selectivity sequence at low  $[\text{Ca}^{2+}]_o$ , notable for a very low permeability to  $\text{Cs}^+$  from either side of the membrane. Typical voltage-activated  $\text{Ca}^{2+}$  channels lose their ionic selectivity when extracellular  $\text{Ca}^{2+}$  is lowered, becoming permeable to monovalent ions including  $\text{Na}^+$ ,  $\text{Li}^+$ ,  $\text{K}^+$ ,  $\text{Rb}^+$ , and  $\text{Cs}^+$  (McCleskey and Almers, 1985; Hess et al., 1986). Although the high selectivity for  $\text{Ca}^{2+}$  over monovalents at high  $[\text{Ca}^{2+}]_o$  points to a multi-

ion selectivity filter similar to other  $\text{Ca}^{2+}$  channels,  $I_{\text{CRAC}}$  channels show a high ionic selectivity even at micromolar external  $\text{Ca}^{2+}$ , when the selectivity for divalent ions is lost. Both the reversal potential and the mean currents show a high selectivity for  $\text{Na}^+$  over  $\text{Cs}^+$  under these conditions. We propose that the  $I_{\text{CRAC}}$  channel pore is considerably smaller than the pore of a typical voltage-gated  $\text{Ca}^{2+}$  channel, acting as a molecular sieve in addition to the presumed high affinity  $\text{Ca}^{2+}$  binding site.

The study of  $\text{Na}^+$  currents through  $I_{\text{CRAC}}$  channels provides an enhanced current model permitting the examination of single channel characteristics. Observing currents in the virtual absence of  $\text{Ca}^{2+}$  allows separation of complicated  $\text{Ca}^{2+}$  dependent activation- inactivation mechanisms, several of which have been described to be involved in the regulation of this physiologically important channel.

We thank Diana Cooper and Dr. Lu Forrest for assistance with cell culture. This work was supported by National Institutes of Health grants NS14609 and GM41514, and by a fellowship from the Deutsche Forschungsgemeinschaft (Le 792/2).

## REFERENCES

- Almers, W., E. W. McCleskey, and P. T. Palade. 1984. A non-selective cation conductance in frog muscle membrane blocked by micromolar external calcium ions. *J. Physiol.* 353:565–583.
- Ellinor, P. T., J. Yang, W. A. Sather, J. F. Zhang, and R. W. Tsien. 1995.  $\text{Ca}^{2+}$  channel selectivity at a single locus for high-affinity  $\text{Ca}^{2+}$  interactions. *Neuron.* 15:1121–1132.
- Fasolato, C., B. Innocenti, and T. Pozzan. 1994. Receptor activated  $\text{Ca}^{2+}$  influx: how many mechanisms for how many channels? *Trends Pharmacol. Sci.* 15:77–83.
- Fasolato, C., M. Hoth, and R. Penner. 1993. A GTP-dependent step in the activation mechanism of capacitative calcium influx. *J. Biol. Chem.* 268:20737–20740.
- Fukushima, Y., and S. Hagiwara. 1985. Currents carried by monovalent cations through calcium channels in mouse neoplastic B lymphocytes. *J. Physiol.* 358:255–284.
- Hess, P., and R. W. Tsien. 1984. Mechanism of ion permeation through calcium channels. *Nature.* 309:453–456.
- Hess, P., J. B. Lansman, and R. W. Tsien. 1986. Calcium channel selectivity for divalent and monovalent cations. Voltage and concentration dependence of single channel current in ventricular heart cells. *J. Gen. Physiol.* 88:293–319.
- Hoth, M. 1995. Calcium and barium permeation through calcium release-activated calcium (CRAC) channels. *Pflügers Arch. Eur. J. Physiol.* 430:315–322.
- Hoth, M., and R. Penner. 1992. Depletion of intracellular calcium stores activates a calcium current in mast cells. *Nature.* 355:353–356.
- Hoth, M., and R. Penner. 1993. Calcium release-activated calcium current in rat mast cells. *J. Physiol.* 465:359–386.
- Lepple-Wienhues, A., and M. D. Cahalan. 1995. Two different calcium-influx pathways in melanoma cells are cell cycle-dependent. *Biophys. J.* 68:A122.
- Lepple-Wienhues, A., and M. D. Cahalan. 1996. Monovalent cation permeation through stores-dependent  $\text{Ca}^{2+}$  channels (Icrac) in Jurkat T lymphocytes. *Biophys. J.* 70:A152.
- Lewis, R. S., and M. D. Cahalan. 1989. Mitogen-induced oscillations of cytosolic  $\text{Ca}^{2+}$  and transmembrane  $\text{Ca}^{2+}$  current in human leukemic T cells. *Cell Regul.* 1:99–112.
- Lewis, R. S., and M. D. Cahalan. 1995.  $\text{Ca}^{2+}$  and  $\text{K}^+$  channels in lymphocytes. *Annu. Rev. Immunol.* 13:623–653.
- Lückhoff, A., and D. E. Clapham. 1994. Calcium channels activated by depletion of internal calcium stores in A431 cells. *Biophys. J.* 67:177–182.
- McCleskey, E. W., and W. Almers. 1985. The Ca channel in skeletal muscle is a large pore. *Proc. Natl. Acad. Sci. USA.* 82:7149–7153.
- McDonald, T. V., B. A. Premack, and P. Gardner. 1993. Flash photolysis of caged inositol 1,4,5-trisphosphate activates plasma membrane calcium current in human T cells. *J. Biol. Chem.* 268:3889–3896.
- Negulescu, P. A., N. Shastri, and M. D. Cahalan. 1994. Intracellular calcium dependence of gene expression in single T lymphocytes. *Proc. Natl. Acad. Sci. USA.* 91:2873–2877.
- Neher, E. 1988. The influence of intracellular  $\text{Ca}^{2+}$  concentration on degranulation of dialyzed mast cells from rat peritoneum. *J. Physiol.* 395:193–214.
- Parekh, A. B., H. Terlau, and W. Stühmer. 1993. Depletion of  $\text{InsP}_3$  stores activates a  $\text{Ca}^{2+}$  and  $\text{K}^+$  current by means of a phosphatase and a diffusible messenger. *Nature.* 364:814–818.
- Parekh, A. B., and R. Penner. 1995. Depletion-activated calcium current is inhibited by protein kinase in RBL-2H3 cells. *Proc. Natl. Acad. Sci. USA.* 92:7907–7911.
- Premack, B. A., T. V. McDonald, and P. Gardner. 1994. Activation of  $\text{Ca}^{2+}$  current in Jurkat T cells following the depletion of  $\text{Ca}^{2+}$  stores by microsomal  $\text{Ca}^{2+}$ -ATPase inhibitors. *J. Immunol.* 152:5226–5240.
- Randriamampita, C., and R. Y. Tsien. 1993. Emptying of intracellular  $\text{Ca}^{2+}$  stores releases a novel small messenger that stimulates  $\text{Ca}^{2+}$  influx. *Nature.* 364:809–814.
- Ross, P. E., and M. D. Cahalan. 1995.  $\text{Ca}^{2+}$  influx pathways mediated by swelling or stores depletion in mouse thymocytes. *J. Gen. Physiol.* 106:415–444.
- Somasundaram, B., J. C. Norman, and M. P. Mahaut-Smith. 1995. Primaquine, an inhibitor of vesicular transport, blocks the calcium-release-activated current in rat megakaryocytes. *Biochem. J.* 309:725–729.
- Vaca, L., and D. L. Kunze. 1994. Depletion of intracellular  $\text{Ca}^{2+}$  stores activates a  $\text{Ca}^{2+}$  selective channel in vascular endothelium. *Am. J. Physiol.* 267:C920–C925.
- Zhang, L., and M. A. McCloskey. 1995. Immunoglobulin E receptor-activated calcium conductance in rat mast cells. *J. Physiol.* 483:59–66.
- Zweifach, A., and R. S. Lewis. 1993. Mitogen-regulated  $\text{Ca}^{2+}$  current of T lymphocytes is activated by depletion of intracellular  $\text{Ca}^{2+}$  stores. *Proc. Natl. Acad. Sci. USA.* 90:6295–6299.
- Zweifach, A., and R. S. Lewis. 1995a. Rapid inactivation of depletion-activated calcium current ( $I_{\text{CRAC}}$ ) due to local calcium feedback. *J. Gen. Physiol.* 105:209–226.
- Zweifach, A., and R. S. Lewis. 1995b. Slow calcium-dependent inactivation of depletion-activated calcium current. Store-dependent and -independent mechanisms. *J. Biol. Chem.* 270:14445–14451.
- Zweifach, A., and R. S. Lewis. 1996. Calcium-dependent potentiation of store-operated calcium channels in T lymphocytes. *J. Gen. Physiol.* 107:597–610.